Submitted to the 2016 IEEE American Control Conference, July 6-8, Boston, MA, USA

Adaptive Output-Feedback Control for A Class of Multi-Input-Multi-Output Plants with Applications to Very Flexible Aircraft*

Zheng Qu[1], Anuradha M. Annaswamy[1] and Eugene Lavretsky[2]

***Abstract*— A dominant presence of parametric model uncertainties necessitates an adaptive approach for control of very flexible aircraft (VFA). This paper proposes an adaptive controller that includes a baseline design based on observers and parameter adaptation based on a closed-loop reference model (CRM), and is applicable for a class of multi-input multi-output (MIMO) plants where number of outputs exceeds number of inputs. In particular, the proposed controller allows the plant to have first-order actuator dynamics and parametric uncertainties in both plant and actuator dynamics. Conditions are delineated under which this controller can guarantee stability and asymptotic reference tracking, and the overall design is validated using simulations on a nonlinear VFA model.**

I. Introduction

Very Flexible Aircraft (VFA) corresponds to an aerial platform whose equilibrium flight conditions (*trim*s) critically depend on its flexible wing shape [1], [2], and has been investigated as a potential solution to generate high-altitude low-endurance (HALE) flights [2]. One of the challenges of VFA is a significant change in its rigid-body dynamics when the flexible wing deforms. For example, the pitch (short period) mode of VFA can become unstable when wing dihedral is trimmed at a high value [1], [3]. As a consequence, control designs based on rigid-body dynamics only may fail to stabilize the aircraft [3].

Nonlinear VFA models have been investigated in [1], [4], [5] with focus on capturing the flexibility effects as well as on advanced control designs. A particular control challenge for VFA is that only rigid body state measurements are available for control, while wing flexible states are not. Another control challenge is that maneuvers of VFA requires navigation through multiple trims, which necessitates additional gain scheduling design. This paper proposes an adaptive output-feedback controller together with gain scheduling.

The classical approach to MIMO adaptive controllers (see [6, Chapter 10] and [7, Chapter 9]) is based on the underlying plant transfer function matrix. Such a design typically requires the knowledge of plant's Hermite form [8], [9] and uses a non-minimal observer along with a reference model. In contrast to the classical method, recent literature proposes a new approach based on state-space representation, which uses a minimal observer to generate the underlying state estimates [10]–[14, Chapter 14]. Unlike the classical approach, the minimal observer is also used as a reference model, by appealing to the notion of a CRM, which is recently shown to be a highly promising direction in adaptive control due to improved transients [15]. The controllers proposed in these references, however, are based on a restrictive assumption that the underlying relative degree of the plant is uniformly unity, which ignore any actuator dynamics that may be present. While this was relaxed in [16] to include a relative-degree two plant, some of the assumptions made regarding the parametric uncertainties therein prevents the application of the proposed controller to VFA models. In this paper, we relax these assumptions. In particular, we assume that the plant may be non-square, allow a larger class of parametric uncertainties, and include actuator dynamics that may be unknown.

This paper is organized as follows. Section II introduces mathematical preliminaries. Section III formulates the control problem in the context of VFA control. Section IV develops an adaptive controller and presents the stability analysis. Section V presents simulation results.

II. Preliminaries

Consider a MIMO plant model $\{A, B, C\}$ with m inputs and m outputs. The notation $\{A, B, C\}$ is defined as $\{A, B, C\} = G(s) = C(sI - A)^{-1}B$. The transmission zeros of the plant model is defined as following.

Definition 1. [17] For a non-degenerate m-input and p-output linear system with minimal realization (A, B, C), the transmission zeros are defined as the finite values of s such that $rank[R(s)] < n + \min(m, p)$, where $R(s) = \begin{bmatrix} sI - A & B \\ C & 0 \end{bmatrix}$.

We part B into columns as $B = \begin{bmatrix} b_1, & b_2, & \cdots, & b_m \end{bmatrix}$ with b_i corresponding to the ith input u_i. The input relative degree of the plant model is defined as following.

Definition 2. A linear square plant model $\{A, B, C\}$ has

a) input relative degree $\mathfrak{r} = \begin{bmatrix} r_1, & r_2, & \cdots, & r_m \end{bmatrix}^T \in \mathbb{N}^{m\times 1}$ if and only if

$$i) \quad \forall j \in \{1, \cdots, m\},\ \forall k \in \{0, \cdots, r_j - 2\}\ : \quad CA^k b_j = 0_{m\times 1}, \quad \text{and} \tag{1}$$

$$ii) \quad rank \begin{bmatrix} CA^{r_1-1}b_1 & CA^{r_2-1}b_2 & \cdots & CA^{r_2-1}b_m \end{bmatrix} = m; \tag{2}$$

* This work is supported by Boeing Strategic University Initiative.

1. Department of Mechanical Engineering, Massachusetts Institute of Technology, Cambridge, MA 02139, USA.

2. The Boeing Company, Huntington Beach, CA, 92647, USA.

b) uniform input relative degree $r \in \mathbb{N}$ if and only if it has input relative degree $\mathfrak{r} = \begin{bmatrix} r_1, & r_2, & \cdots, & r_m \end{bmatrix}^T$ and $r = r_1 = r_2 = \cdots = r_m$.

c) nonuniform input relative degree $\mathfrak{r} \in \mathbb{N}^m$ if and only if it has input relative degree $\mathfrak{r} = \begin{bmatrix} r_1, & r_2, & \cdots, & r_m \end{bmatrix}^T$ and $r_i \neq r_j$ for some $i, j \in 1, 2, \cdots, m$ and $i \neq j$.

For $G(s)$ to have input relative degree, u_i should start to have nonzero (and linearly independent) contribution towards the r_ith derivative of at least one output in y. Generically, any MIMO plant model has input relative degree since condition $i)$ and $ii)$ are generically satisfied.

III. Problem Statement

Our starting point is a nonlinear VFA model including its complete rigid body dynamics and flexible component dynamics as derived in [5] using the virtual work method, assuming control surfaces are on the flexible components:

$$\begin{bmatrix} M_{FF} & M_{FB} \\ M_{BF} & M_{BB} \end{bmatrix} \begin{bmatrix} \ddot{\epsilon} \\ \dot{\beta} \end{bmatrix} + \begin{bmatrix} C_{FF} & C_{FB} \\ C_{BF} & C_{BB} \end{bmatrix} \begin{bmatrix} \dot{\epsilon} \\ \beta \end{bmatrix} + \begin{bmatrix} K_{FF} & 0 \\ 0 & 0 \end{bmatrix} \begin{bmatrix} \epsilon \\ b \end{bmatrix} = \begin{bmatrix} B_F \\ B_B \end{bmatrix} F^{aero}. \quad (3)$$

$\epsilon = \begin{bmatrix} \epsilon_1^T, & \epsilon_2^T, & \epsilon_3^T, & \cdots, & \epsilon_{n_f}^T \end{bmatrix}^T$ are states of the flexible wing with ϵ_i being states of each discretized flexible segments and $\dot{b} = \beta = \begin{bmatrix} v_B^T & \omega_B^T \end{bmatrix}^T$ are states of rigid body with v_B being linear velocities and ω_B being angular velocities. The model is derived by discretizing the flexible wing into n_f components, each of which has 6 degree of freedom and has compliant joints with its neighboring components. K_{FF} is the stiffness of the joints. Define $J_{h\epsilon} = \frac{\partial h}{\partial \epsilon}$ and $J_{hb} = \frac{\partial h}{\partial b}$ as the Jacobian matrices with $h(\epsilon(r), b) := \begin{bmatrix} p^T(r) & w^T(r) \end{bmatrix}^T$ being local positions and orientations of discretized elements, and r being local wing coordinate. After summation of their local values at each component along the r direction, the Jacobian matrices and the inertia matrices $M_{(\cdot)(\cdot)}$ become functions of ϵ and b only. In addition, since $\dot{J}_{h\epsilon} = \frac{\partial^2 h}{\partial^2 \epsilon}\dot{\epsilon} + \frac{\partial^2 h}{\partial \epsilon \partial b}\dot{b}$ and $\dot{J}_{hb} = \frac{\partial^2 h}{\partial b \partial \epsilon}\dot{\epsilon} + \frac{\partial^2 h}{\partial^2 b}\dot{b}$, the compliance matrices $C_{(\cdot)(\cdot)}$ are functions of $\epsilon, \dot{\epsilon}, b, \beta$. More specifically [5],

$$\begin{gathered} M_{FF}(\epsilon) = J_{h\epsilon}^T M_e J_{h\epsilon}, \quad M_{BF}(\epsilon) = J_{hb}^T M_e J_{h\epsilon} \\ M_{FB}(\epsilon) = J_{h\epsilon}^T M_e J_{hb}, \quad M_{BB}(\epsilon) = J_{hb}^T M_e J_{hb} + M_{RB} \\ C_{FF}(\epsilon, \dot{\epsilon}, \beta) = J_{h\epsilon}^T M_e \dot{J}_{h\epsilon} + C_e \\ C_{BF}(\epsilon, \dot{\epsilon}, \beta) = J_{hb}^T M_e \dot{J}_{h\epsilon} \\ C_{FB}(\epsilon, \dot{\epsilon}, \beta) = J_{h\epsilon}^T M_e \Omega_B J_{hb} + 2 J_{h\epsilon}^T M_e \dot{J}_{hb} \\ C_{BB}(\epsilon, \dot{\epsilon}, \beta) = J_{hb}^T M_e \Omega_B J_{hb} + 2 J_{hb}^T M_e \dot{J}_{hb} + C_{RB} \\ B_F(\epsilon) = J_{h\epsilon}, \quad B_B(\epsilon) = J_{hb} \\ F^{aero} = F^{aero}(\ddot{\epsilon}, \dot{\epsilon}, \epsilon, \dot{\beta}, \beta, u_s) \end{gathered} \quad (4)$$

where M_e is the effective flexible component inertia and M_{RB} is the rigid body inertia; C_e is the effective flexible component compliance, C_{RB} is the rigid body compliance, u_s is the control surface input, and Ω_B is a matrix associated with coordinate rotation effects (see [5]). Further, we assume that inertia and compliance properties of flexible components vary slowly with respect to the rigid body positions and orientations. As a result, $J_{(\cdot)(\cdot)}$, $M_{(\cdot)(\cdot)}$ and $B_{(\cdot)}$ are only function of ϵ, and the compliance matrices $C_{(\cdot)(\cdot)}$ are only functions of $\epsilon, \dot{\epsilon}, \beta$. The generalized aerodynamic loading F^{aero} are calculated at each local flexible component using the 2-D finite inflow theory [5], and then summed along the r direction. It is noted that because inertia, compliance and external load effects are all subject to local coordinate transformation, $M_{(\cdot)(\cdot)}$, $C_{(\cdot)(\cdot)}$ and $B_{(\cdot)}$ all have J_{hb} or $J_{h\epsilon}$ as their leading factors.

To design a controller for a trim $\begin{bmatrix} \ddot{\epsilon}_0 & \dot{\epsilon}_0 & \epsilon_0 & \dot{\beta}_0 & \beta_0 & u_0 \end{bmatrix}^T$, we define deviation states and inputs as $x_p = \begin{bmatrix} \epsilon - \epsilon_0 & \dot{\epsilon} - \dot{\epsilon}_0 & \beta - \beta_0 \end{bmatrix}^T \in \mathbb{R}^{n_p}$ and $u_p = (u_s - u_0) \in \mathbb{R}^m$, respectively, and perform model linearization (ignoring high-order error terms) as

$$\begin{aligned} &Q_1(\ddot{\epsilon}_0, \dot{\epsilon}_0, \epsilon_0, \dot{\beta}_0, \beta_0, u_0)\dot{x}_p \\ &\quad = Q_2(\ddot{\epsilon}_0, \dot{\epsilon}_0, \epsilon_0, \dot{\beta}_0, \beta_0, u_0)x_p + Q_3(\epsilon_0, \beta_0, u_0)u_p, \end{aligned} \quad (5)$$

where Q_1 includes inertia matrices, and Q_2 includes compliance and stiffness matrices (see Appendix A for detail derivations). Assuming Q_1^{-1} exists, Eq.(5) leads to $\dot{x}_p = Q_1^{-1}Q_2 x_p + Q_1^{-1}Q_3 u_p$, which is linear time invariant (LTI) around a single trim but becomes linear parameter varying (LPV) when the aircraft navigates through trims. Control of the LPV plant requires gain scheduling [18] with respect to $(\ddot{\epsilon}_0, \dot{\epsilon}_0, \epsilon_0, \dot{\beta}_0, \beta_0, u_0)$, which faces difficulties since only $(\epsilon_0, \beta_0, u_0)$ are measurable, while $(\ddot{\epsilon}_0, \dot{\epsilon}_0, \dot{\beta}_0)$ are not. The controller has to schedule its gains using an assumed trim point, which introduces model uncertainties into (5) as

$$\begin{aligned} &\Big[Q_1(0,0,\epsilon_0,0,\beta_0,u_0) + \Delta Q_1(\ddot{\epsilon}_0, \dot{\epsilon}_0, \dot{\beta}_0)\Big]\dot{x}_p = \\ &\qquad \Big[Q_2(0,0,\epsilon_0,0,\beta_0,u_0) + \Delta Q_2(\ddot{\epsilon}_0, \dot{\epsilon}_0, \dot{\beta}_0)\Big]x_p \\ &\qquad\qquad + Q_3(\epsilon_0, \beta_0, u_0)u_p \end{aligned} \quad (6)$$

where ΔQ_1 and ΔQ_2 are functions of $(\ddot{\epsilon}_0, \dot{\epsilon}_0, \dot{\beta}_0)$ and therefore unknown. Further examination reveals that ΔQ_1 and ΔQ_2 can be written as (see Appendix A)

$$\Delta Q_1 = Q_3 \Theta_{q_1}^{*T}, \quad \Delta Q_2 = Q_3 \Theta_{q_2}^{*T}. \quad (7)$$

where $\Theta_{q_1}^{*T}$ and $\Theta_{q_2}^{*T}$ are function of $(\ddot{\epsilon}_0, \dot{\epsilon}_0, \dot{\beta}_0)$. Eq.(7) implies that the local body inertia and compliance changes caused by wing deformation can be approximated by similar changes caused by external loads. We assume Q_1, $(Q_1 + Q_3\Theta_{q_1}^{*T})$ and $(I + \Theta_{q_2}^{*T} Q_1^{-1} Q_3)$ are always invertible. Using (7) and taking inverse on both sides, (6) becomes

$$\begin{gathered} \dot{x}_p = (A_p + B_p \Theta_p^{*T}) x_p + B_p \Lambda^* u_p \\ y_p = C_p x_p \\ z = (C_{pz} + D_z \Theta_p^{*T}) x_p + D_z \Lambda^* u_p \end{gathered} \quad (8)$$

where $A_p(\epsilon_0, \beta_0, u_0) = Q_1^{-1}Q_2$, $B_p(\epsilon_0, \beta_0, u_0) = Q_1^{-1}Q_3$, $\Theta_p^{*T}(\ddot{\epsilon}_0, \dot{\epsilon}_0, \dot{\beta}_0) = \Theta_{q_2}^{*T} - \overline{\Theta}_{q_1}^{*T} A_p - \overline{\Theta}_{q_1}^{*T} B_p \Theta_{q_2}^{*T}$, $\Lambda^*(\ddot{\epsilon}_0, \dot{\epsilon}_0, \dot{\beta}_0) = \Lambda_p^* \Lambda_d^*$, $\Lambda_p^*(\ddot{\epsilon}_0, \dot{\epsilon}_0, \dot{\beta}_0) = (I - \overline{\Theta}_{q_1}^{*T} B_p)$ and $\overline{\Theta}_{q_1}^{*T}(\ddot{\epsilon}_0, \dot{\epsilon}_0, \dot{\beta}_0) = (I + \Theta_{q_1}^{*T} Q_1^{-1} Q_3)^{-1} \Theta_{q_1}^{*T}$ (see Appendix A for detail derivations). The constant matrix Λ_d^* represents loss

of control effectiveness due to possible damage to the control surfaces. $y \in \mathbb{R}^p$ are measurement outputs and $z \in \mathbb{R}^r$ are tracking outputs. The numbers of inputs and outputs satisfies $p + r > m$. Matrices $A_p \in \mathbb{R}^{n_p \times n_p}$, $B_p \in \mathbb{R}^{n_p \times m}$, $C_p \in \mathbb{R}^{p \times n_p}$, $B_{pz} = \mathbb{R}^{n_p \times r}$, $C_{pz} \in \mathbb{R}^{r \times n_p}$ and $D_z \in \mathbb{R}^{r \times m}$ are functions of $(\epsilon_0, \beta_0, u_0)$ and are known. $\Theta_p^* \in \mathbb{R}^{n_p \times m}$ and $\Lambda^* \in \mathbb{R}^{m \times m}$ are functions of $(\ddot{\epsilon}_0, \dot{\epsilon}_0, \dot{\beta}_0)$ and are unknown.

Eq.(8) is the actual uncertain LPV plant model when the controller performs gain scheduling. All matrices in Eq.(8) are assumed to vary slowly between trims and Eq.(8) are treated as an uncertain LTI plant when we design control parameters around a single trim.

(A_p, B_p, C_p) is assumed to be a minimal realization and have stable transmission zeros. It is also assumed that $C_p B_p$ has full column rank and therefore the plant model has uniform input relative degree one (see [14] for a justifications of these assumptions). Adaptive control design for (A_p, B_p, C_p) (referred as relative degree one adaptive controller hereafter) has been developed in Ref. [10], [11], [14] and is able to achieve asymptotic tracking of a reference trajectory for z.

In this paper, we introduce uncertain first order actuator dynamics in each input, which is modeled as $\dot{u}_p + c(I + \Theta_a^{*T})u_p = cu$ where $\Theta_a^* \in \mathbb{R}^{m \times m}$ represents the uncertainties in actuator time constants. Define $w_u = \Lambda^* u_p$ and rewrite the actuator dynamics as $\dot{w}_u + c(1 + \overline{\Theta}_a^{*T})w_u = c\Lambda^* u$ with $\overline{\Theta}_a^{*T} = \Lambda^* \Theta_a^{*T} \Lambda^{*-1}$. For command tracking, we also augment the LTI plant with integral error states $w_{pz} := \int (z - z_{cmd}) dt$, as shown in Eq.(9), which is rewritten in a compact form as

$$\begin{gathered} \dot{x} = Ax + B_1 \Psi_1^{*T} x + B_2 \Psi_2^{*T} x + B_2 \Lambda^* u + B_z z_{cmd} \\ y = Cx \\ z = C_z x + D_z \Psi_1^{*T} x. \end{gathered} \tag{10}$$

$x \in \mathbb{R}^n$ are augmented states, $u \in \mathbb{R}^m$ are new control inputs, $y \in \mathbb{R}^m$ are augmented measurement outputs. Matrices $A \in \mathbb{R}^{n \times n}$, $B_1 \in \mathbb{R}^{n \times m}$, $B_2 \in \mathbb{R}^{n \times m}$, $C \in \mathbb{R}^{m \times n}$, $B_z = \mathbb{R}^{n \times r}$, $C_z \in \mathbb{R}^{r \times n}$ and $D_z \in \mathbb{R}^{r \times m}$ are known. Uncertainty matrices have the form of $\Psi_1^{*T} = \begin{bmatrix} \Theta_p^{*T} & 0 & 0 \end{bmatrix} \in \mathbb{R}^{m \times n}$, $\Psi_2^{*T} = \begin{bmatrix} 0 & \overline{\Theta}_a^{*T} & 0 \end{bmatrix} \in \mathbb{R}^{m \times n}$, $\Lambda^* \in \mathbb{R}^{m \times m}$ and are unknown constants. $B_1 \Psi_1^{*T}$ are uncertainties in the plant dynamics and $B_2 \Psi_2^{*T}$ are the uncertainties in the actuator dynamics. The control goal is to design u such that z tracks a trajectory z_m from a reference model. The adaptive controller that we will present requires the following assumptions regarding the plant model (10) to be valid around each trim:

Assumption 1. *(A, B_2, C) is a minimal realization;*

Assumption 2. *All $\{A, B_2, C\}$'s transmission zeros (a total of n_z) are stable;*

Assumption 3. *$\{A, B_2, C\}$ has uniform relative degree two and satisfies $(n - n_z - 2m) \geq (p - m)$;*

Assumption 4. *B_1 can be spanned by a linear combination of B_2 and AB_2, and Ψ_1^* satisfies $\Psi_1^{*T} B_2 = 0$;*

Assumption 5. *Ψ_1^* and Ψ_2^* are bounded by a known value, i.e. $\|\Psi_1^*\| < \Psi_{max}^*$ and $\|\Psi_2^*\| < \Psi_{max}^*$;*

Assumption 6. *Λ^* is symmetric positive definite and bounded by a known value, i.e. $\|\Lambda^*\| < \Lambda_{max}$.*

Assumption 1 and 2 is always satisfied if (A_p, B_p, C_p) is a minimal realization and has stable transmission zeros. The fact that (A, B_2, C) is non-square and typically has no transmission zeros [19] makes Assumption 2 reasonable. Assumption 4 is always satisfied if the plant model has the structure as in (9), in which case $B_1 = \frac{1}{c} A B_2 + B_2$. For nominal plant models satisfying Assumptions 1 and 2, a baseline observer-based controller (such as LQG [20]) with gain scheduling can be designed to achieve a satisfactory tracking performance with adequate stability margins.

For adaptive control, additional assumptions on the plant model are needed. For (9), Assumption 3 implies $\begin{bmatrix} C_p B_p \\ D_z \end{bmatrix}$ has column rank m (see [16] for relaxation to nonuniform relative degree cases). The inequality $(n - n_z - 2m) \geq (p - m)$ allows a squaring-up method to be carried out. Assumption 5 is commonly satisfied for aerial platforms with physical constrains, such as the maximum allowable deformation rate in VFA. Assumption 6 is satisfied if $\Theta_{q_1}^{*T}$ has a small magnitude, which implies that inertia properties of aircraft varies slowly, and Λ_d^* is positive definite and diagonal, which implies that control effectiveness loss is independent from each other.

IV. Adaptive Output-Feedback Control

This section will develop an adaptive controller for relative degree two LTI plant models. In Section IV-A, a squaring-up procedure is introduced to produce a square plant model. A special state coordinate suitable for control design is presented in Section IV-B. The adaptive controller is developed in Section IV-C and its parameters are designed in Section IV-D to guarantee SPR properties of an underlying SPR error model shown in Section IV-E. Adaptive law and stability analysis can be found in Section IV-F.

A. Squaring-Up

The new adaptive control design will be based on a square plant model, which necessitates a squaring-up procedure being carried out on (A, B_2, C). Lemma 3 specify the details of the squaring-up procedure, whose proof can be found in [21]. Define $m_s := p - m$.

Lemma 3. *For plant models satisfying Assumptions 1 to 3, there exists a $B_{s1} \in \mathbb{R}^{n \times m_s}$ such that $(A, \overline{B}_2, C)$, where $\overline{B}_2 = \begin{bmatrix} B_2 & B_{s1} \end{bmatrix}$, has stable transmission zeros and nonuniform input relative degree $r_i = 2$ for $i = 1, 2, \cdots, m$ and $r_i = 1$ for $i = m+1, m+2, \cdots, p$.*

Similar to $\overline{B}_2$, we part $C^T = \begin{bmatrix} C_2^T & C_1^T \end{bmatrix}$. In the following design procedures, we will show that B_{s1} will only be used to design control parameters.

B. Input Normal Form

For a square plant model that has nonuniform input relative degree two, there exists an invertible transformation $T_{in} = \begin{bmatrix} (\mathfrak{C}\mathfrak{B})^{-1}\mathfrak{C} \\ \mathfrak{N} \end{bmatrix}$, $T_{in}^{-1} = \begin{bmatrix} \mathfrak{B} & \mathfrak{M} \end{bmatrix}$, where $\mathfrak{C}^T =$

$$\begin{bmatrix} \dot{x}_p \\ \dot{w}_u \\ \dot{w}_z \end{bmatrix} = \underbrace{\begin{bmatrix} A_p & B_p & 0 \\ 0 & -cI & 0 \\ C_{pz} & D_z & 0 \end{bmatrix}\begin{bmatrix} x_p \\ w_u \\ w_z \end{bmatrix}}_{A\quad x} + \underbrace{\begin{bmatrix} B_p \\ 0 \\ D_z \end{bmatrix}}_{B_1}\Lambda^*\Theta_p^{*T}x_p + \underbrace{\begin{bmatrix} 0 \\ cI \\ 0 \end{bmatrix}}_{B_2}\Lambda^*\left[u + \Theta_a^{*T}\Lambda^{*-1}w_u\right] + \underbrace{\begin{bmatrix} 0 \\ 0 \\ -I \end{bmatrix}}_{B_z} z_{cmd}$$
$$y = \underbrace{\begin{bmatrix} C_p & 0 & 0 \\ 0 & 0 & I \end{bmatrix}}_{C} x, \quad z = \underbrace{\begin{bmatrix} C_{pz} & D_z & 0 \end{bmatrix}}_{C_z} x + D_z\Lambda^*\Theta_p^{*T}x_p. \tag{9}$$

$\begin{bmatrix} C_2^T & A^TC_2^T & C_1 \end{bmatrix}$, $\mathfrak{B} = \begin{bmatrix} B_2 & AB_2 & B_{s1} \end{bmatrix}$, $\mathfrak{N}$ and $\mathfrak{M}$ are chosen to satisfy $\mathfrak{N}\mathfrak{B} = 0$, $\mathfrak{C}\mathfrak{M} = 0$ and $\mathfrak{N}\mathfrak{M} = I$, that transforms (10) into a new coordinate called "*input normal form*" (See [22, Corollary 2.2.5] for proof). In this paper, matrices in input normal form coordinate will be denoted with the subscript $(\cdot)_{in}$, as in $x_{in} = T_{in}x$, $A_{in} = T_{in}AT_{in}^{-1}$, $\overline{B}_{2,in} = T_{in}\overline{B}_2$ (and therefore $B_{2,in} = T_{in}B_2$ and $B_{s1,in} = T_{in}B_{s1}$), $B_{1,in} = T_{in}B_1$, $B_{in,z} = T_{in}B_z$, $C_{in} = CT_{in}^{-1}$, $\Psi_{1,in}^{*T} = \Psi_1^{*T}T_{in}^{-1}$ and $\Psi_{2,in}^{*T} = \Psi_2^{*T}T_{in}^{-1}$. The input normal form of the plant model (10) is

$$\begin{aligned}
\begin{bmatrix} \dot{\xi}_1^2 \\ \dot{\xi}_2^2 \\ \dot{\xi}_1^1 \\ \dot{\eta} \end{bmatrix} &= \underbrace{\left[\begin{array}{cc|c|c} 0 & R_{2,1}^2 & R_{2,1}^1 & V_2 \\ I & R_{2,2}^2 & R_{2,2}^1 & 0 \\ \hline 0 & R_{1,1}^2 & R_{1,1}^1 & V_1 \\ \hline 0 & U_2 & U_1 & Z \end{array}\right]}_{A_{in}}\underbrace{\begin{bmatrix} \xi_1^2 \\ \xi_2^2 \\ \xi_1^1 \\ \eta \end{bmatrix}}_{x_{in}} + \underbrace{\begin{bmatrix} I_m \\ 0 \\ 0 \\ 0 \end{bmatrix}}_{B_{2,in}}\Lambda^* u \\
&\quad + B_{2,in}\underbrace{\begin{bmatrix} \psi_{20}^{2*T} & \psi_{21}^{2*T} \mid \psi_{21}^{1*T} \mid \psi_{(n-r_s)}^{2*T} \end{bmatrix}}_{\Psi_{1,in}^{*T}}x_{in} \\
&\quad + \underbrace{\begin{bmatrix} I_m \\ \frac{1}{c}I_m \\ 0 \\ 0 \end{bmatrix}}_{B_{1,in}}\underbrace{\begin{bmatrix} 0 & \psi_{11}^{2*T} \mid \psi_{11}^{1*} \mid \psi_{(n-r_s)}^{1*T} \end{bmatrix}}_{\Psi_{1,in}^{*T}}x_{in} + B_{in,z}z_{cmd} \\
y &= \underbrace{\begin{bmatrix} 0 & CAB_2 \mid CB_{s1} \mid 0 \end{bmatrix}}_{C_{in}}x_{in}.
\end{aligned} \tag{11}$$

Matrix $Z \in \mathbb{R}^{(n-r_s)\times(n-r_s)}$, where $r_s = \sum_i r_i$, is the zero dynamics matrix whose eigenvalues are transmission zeros of the plant model (see [22, Section 2.3]). The norms of $\Psi_{1,in}^{*T}$ and $\Psi_{2,in}^{*T}$ are bounded by known values as

$$\left\|\Psi_{i,in}^*\right\| \le \overline{\Psi}_{max} \quad \overline{\Psi}_{max} := \Psi_{max}\left\|T_{in}^{-1}\right\|, \ i = 1, 2. \tag{12}$$

It is noted that $B_{1,in} = \begin{bmatrix} \times & \times & 0 & 0 \end{bmatrix}^T$ and $\Psi_1^{*T}T_{in}^{-1} = \begin{bmatrix} 0 & \times & \times & \times \end{bmatrix}$ since Assumption 4 holds.

Define $A_{in}^* = A_{in} + B_{1,in}\Psi_{1,in}^{*T} + B_{2,in}\Psi_{2,in}^{*T}$. Suppose we add differentiators to all inputs in u, i.e. $a_1^1\dot{v} + a_1^0 v = u$. We then are able to manufacture an artificial uniform relative degree one square plant model $\{A_{in}^*, \overline{B}_{in}^{1*}, C_{in}\}$ with $u^T = [v^T, u_{s1}^T]$ as inputs, where

$$\begin{aligned}
\overline{B}_{2,in}^{1*} = \begin{bmatrix} B_{2,in}^{1*} & B_{s1,in} \end{bmatrix} &= \left[\begin{array}{cc} a_1^0 I_m + a_1^1\psi_{20}^{2*T} & 0 \\ a_1^1 I_m & 0 \\ \hline 0 & I_{m_s} \\ \hline 0 & 0 \end{array}\right], \\
B_{2,in}^{1*} &= A_{in}^* B_{2,in}a_1^1 + B_{2,in}a_1^0.
\end{aligned} \tag{13}$$

It is noted that $\overline{B}_{2,in}^{1*}$ includes uncertainties because of the presence of $\Psi_{i,in}^{*T}$. The counterpart of $\overline{B}_{2,in}^{1*}$ in the absence of $\Psi_{i,in}^{*T}$ is

$$\begin{aligned}
\overline{B}_{2,in}^{1} = \begin{bmatrix} B_{2,in}^{1} & B_{s1,in} \end{bmatrix} &= \left[\begin{array}{cc} a_1^0 I_m & 0 \\ a_1^1 I_m & 0 \\ \hline 0 & I_{m_s} \\ \hline 0 & 0 \end{array}\right], \\
B_{2,in}^{1} &= A_{in}B_{2,in}a_1^1 + B_{2,in}a_1^0.
\end{aligned} \tag{14}$$

It is noted that $C_{in}\overline{B}_{2,in}^1 = C_{in}\overline{B}_{2,in}^{1*} = \begin{bmatrix} a_1^1 CAB_2 & CB_{s1} \end{bmatrix}$ has full rank by Assumption 3 and Lemma 3. Examination shows that $\overline{B}_{2,in}^{1*}$ and $\overline{B}_{2,in}^1$ satisfies

$$\overline{B}_{2,in}^{1*} = \overline{B}_{2,in}^1 + B_{2,in}a_1^1\Psi_{in,m}^{*T}. \tag{15}$$

where

$$\Psi_{in,m}^{*T} = \begin{bmatrix} \psi_{20}^{2*T} & 0_{m\times m_s} \end{bmatrix} \in \mathbb{R}^{m\times p} \tag{16}$$

which is a subset of the elements in $\Psi_{2,in}^*$. It is noted that (13) also holds for $(A_{in}^* - L_{in}C_{in})$ for $\forall L_{in} \in \mathbb{R}^{n\times m}$. Variants of (13) and (15) in the original coordinate also hold with definitions of $B_2^{1*} = T_{in}^{-1}B_{2,in}^{1*}$, $B_2^1 = T_{in}^{-1}B_{2,in}^1$, $\overline{B}_2^{1*} = T_{in}^{-1}\overline{B}_{2,in}^{1*}$, and $\overline{B}_2^1 = T_{in}^{-1}\overline{B}_{2,in}^1$. The above discussions illustrate the concept of adding zeros, which will be explored in the following control design.

C. Control Architecture

Define s as the differential operator. We choose the control input u as

$$u = u_{bl} + u_{ad} \tag{17}$$

where u_{bl} is determined using a baseline observer-based controller and u_{ad} by an adaptive controller. The baseline control u_{bl} is chosen as

$$u_{bl} = -K^T x_m \tag{18}$$

where $K^T \in \mathbb{R}^{m\times n}$ is designed by the linear quadratic regulator (LQR) technique. u_{ad} is designed as

$$u_{ad} = -u_{bl} + \left(a_1^1 s + a_1^0\right)\Psi_\Lambda^T(t)\chi(t), \tag{19}$$

where $\Psi_\Lambda^T(t) = \begin{bmatrix} \Lambda^T & \Psi_1^T & \Psi_2^T \end{bmatrix}$ and $\overline{\chi}^T = \begin{bmatrix} \overline{u}_{bl}^T & -x_m^T & -\overline{x}_m^T \end{bmatrix}^T$; $\Lambda^T(t) \in \mathbb{R}^{m\times m}$ is an estimate of Λ^{*-1}. $\Psi_1^T(t) \in \mathbb{R}^{m_1\times n}$ and $\Psi_1^T(t) \in \mathbb{R}^{m_1\times n}$ are estimate of $\overline{\Psi}_1^{*T}$ and $\overline{\Psi}_2^{*T}$, respectively, which will be defined in Section IV-E. x_m are the states of a modified closed-loop reference model (CRM, based on Ref. [15]) as

$$\begin{aligned}
\dot{x}_m = Ax_m + B_2u_{bl} + B_2\left(a_1^1 s + a_1^0\right)\left(\Psi_m^T(t)\overline{e}_{ys}\right) \\
+B_z z_{cmd} + L(y - y_m) \\
y_m = Cx_m, \ z_m = C_z x_m + D_z u_{bl}
\end{aligned} \tag{20}$$

where $\Psi_m^T(t) \in \mathbb{R}^{m\times p}$ is an estimate of $\Psi_{in,m}^{*T}$ and

$$e_{ys} := R_{in}^{-1}Se_y, \quad \text{and } e_y := y - y_m. \tag{21}$$

Signals denoted as $\overline{(\cdot)}$ are a filtered version of signals $(\cdot)$ as

$$\begin{aligned}
a_1^1\cdot\dot{\overline{u}}_{bl} + a_1^0\cdot\overline{u}_{bl} = u_{bl} \\
a_1^1\cdot\dot{\overline{x}}_m + a_1^0\cdot\overline{x}_m = x_m \\
a_1^1\cdot\dot{\overline{e}}_{ys} + a_1^0\cdot\overline{e}_{ys} = a_1^1 e_{ys}.
\end{aligned} \tag{22}$$

In (22), $a_1^1, a_1^0 > 0$ are free to design. Control parameters L, R_{in}^{-1} and S will be designed in Section IV-D to guarantee SPR properties of an underlying error model shown in Section IV-E. Adjustable parameters $\Lambda^T(t)$, $\Psi_1^T(t)$, $\Psi_2^T(t)$ and $\Psi_m^T(t)$ will be adapted online by prescribing their derivatives with respect to t, which will be presented in Section IV-F.

D. Design of L and S

The design of L in (20) and S in (21) is performed in the input normal form coordinate and transformed back to the original coordinate, as

$$S = (C_{in}\overline{B}_{2,in}^1)^T, \quad \overline{C}_{in} := SC_{in}, \tag{23}$$

$$\begin{aligned} R_{in}^{-1} = &(\overline{C}_{in}\overline{B}_{2,in}^1)^{-1}[\overline{C}_{in}A_{in}\overline{B}_{2,in}^1 \\ &+ (\overline{C}_{in}A_{in}\overline{B}_{2,in}^1)^T](\overline{C}_{in}\overline{B}_{2,in}^1)^{-1} + \varepsilon I \end{aligned} \tag{24}$$

$$L_{in} = \overline{B}_{2,in}^1 R_{in}^{-1} S_{in}^1, \tag{25}$$

$$L = T_{in}^{-1} L_{in} = \overline{B}_2^1 R_{in}^{-1} S^1. \tag{26}$$

$\varepsilon > 0$ is chosen to be large enough as

$$\varepsilon > \varepsilon_{max}, \quad \varepsilon_{max} = \varepsilon_{max}(A_{in}, \overline{B}_{2,in}^1, \overline{C}_{in}, \overline{\Psi}_{max}) \ . \tag{27}$$

A detail solution of ε_{max} can be found in [16, Eq.(30)]. ε_{max} is so designed to guarantee the SPR properties of an underlying error model as will be shown in the next section.

E. Underlying SPR Error Model

This section will present the underlying error model and its SPR properties. Define

$$L_{in}^* = \overline{B}_{2,in}^{1*} R_{in}^{-1} S_{in}^1, \quad L^* = T_{in}^{-1} L_{in}^* = \overline{B}_2^{1*} R_{in}^{-1} S_{in}^1. \tag{28}$$

It follows (15) that

$$L^* - L = B_2 a_1^1 \Psi_{in,m}^{*T} R_{in}^{-1} S. \tag{29}$$

Define $A^* = A + B_1\Psi_1^{*T} + B_2\Psi_2^{*T}$ and $A_{L^*}^* = A^* - L^*C$. By subtracting (20) from (10), substituting u_{ad} with (19) and L with (29), and appealing to (22)(21), the error model can be derived as

$$\begin{aligned} \dot{e}_x &= A_{L^*}^* e_x + B_2 a_1^1 \Psi_m^{*T} e_{ys} + B_1 \Psi_1^{*T} x_m + B_2 \Psi_2^{*T} x_m \\ &\quad + B_2\Lambda^*(u_{bl} + u_{ad}) - B_2 u_{bl} - B_2\left(a_1^1 s + a_1^0\right)\Psi_m^T(t)\overline{e}_{ys} \\ &= A_{L^*}^* e_x + B_2^{1*}\Lambda^*\overline{\Psi}_1^{*T} x_m + B_2\Lambda^*\overline{\Psi}_2^{*T} x_m \\ &\quad + B_2\Lambda^*\left(a_1^1 s + a_1^0\right)\left[\Lambda^T(t)\overline{u}_{bl} - \Psi_1^T(t)x_m - \Psi_2^T(t)\overline{x}_m\right] \\ &\quad - B_2\left(a_1^1 s + a_1^0\right)\left[\widetilde{\Psi}_m^T(t)\overline{e}_{ys}\right] \\ &= A_{L^*}^* e_x + B_2^{1*}\Lambda^*\overline{\Psi}_1^{*T} x_m - B_2\left(a_1^1 s + a_1^0\right)\left[\widetilde{\Psi}_m^T(t)\overline{e}_{ys}\right] \\ &\quad + B_2\Lambda^*\left(a_1^1 s + a_1^0\right)\left[\widetilde{\Lambda}^T(t)\overline{u}_{bl} - \Psi_1^T(t)x_m - \widetilde{\Psi}_2^T(t)\overline{x}_m\right], \end{aligned} \tag{30}$$

where $\overline{\Psi}_1^{*T} = \Lambda^{*-1}\frac{c}{a_1^1}\Psi_1^{*T}$ and $\overline{\Psi}_2^{*T} = \Lambda^{*-1}\left[\Psi_2^{*T} + \left(I_m - \frac{c}{a_1^1}(a_1^0 I_m + \psi_{20}^{2*T})\right)\Psi_1^{*T}\right]$ are grouped uncertain parameters. Define $e_x' = e_x + B_2\Lambda^* a_1^1 \overline{\Psi}_1^{*T} x_m$. Applying (22)(21) to (30) yields

$$\begin{aligned} \dot{e}_x' = &A_{L^*}^* e_x' - B_2\left(a_1^1 s + a_1^0\right)\left[\widetilde{\Psi}_m^T(t)\overline{e}_{ys}\right] \\ &+ B_2\Lambda^*\left(a_1^1 s + a_1^0\right)\widetilde{\Psi}_\Lambda^T\overline{\chi} \end{aligned} \tag{31}$$

where $\widetilde{\Psi}_\Lambda^T = \begin{bmatrix} \widetilde{\Lambda}^T & \widetilde{\Psi}_1^T & \widetilde{\Psi}_2^T \end{bmatrix}$ with $\widetilde{\Lambda}^T(t) = \Lambda^T(t) - \Lambda^{*-1}$, $\widetilde{\Psi}_1^T(t) = \Psi_1^T(t) - \overline{\Psi}_1^{*T}$, $\widetilde{\Psi}_2^T(t) = \Psi_2^T(t) - \overline{\Psi}_2^{*T}$ and $\widetilde{\Psi}_m^T(t) = \Psi_m^T(t) - \Psi_{in,m}^{*T}$ being parameter estimation errors. Define a new error variable as

$$e_{mx} := e_x' + B_2 a_1^1\left[\widetilde{\Psi}_m^T(t)\overline{e}_{ys}\right] - B_2\Lambda^* a_1^1\widetilde{\Psi}_\Lambda^T\overline{\chi} \tag{32}$$

whose derivatives are found as

$$\dot{e}_{mx} = A_{L^*}^* e_{mx} - B_2^{1*}\widetilde{\Psi}_m^T(t)\overline{e}_{ys} + B_2^{1*}\Lambda^*\widetilde{\Psi}_\Lambda^T\overline{\chi} \tag{33}$$

$$e_y = Ce_{mx} = Ce_x \tag{34}$$

after applying (13). It is noted that (34) holds because $CB_2 = 0$. Eq.s (33) and (34) are our underlying error model.

It is noted that $\{A^*, B_2^{1*}, C\}$ has all stable transmission zeros since we only added m transmission zeros at $-a_1^0/a_1^1$ through filters (22). A formal proof is to write out $\overline{N}_{2,in}^{1*} A_{in}^* M_{in}$ with $M_{in} = \left[\begin{array}{ccc|c} I_m & 0 & 0 & 0 \\ \hline 0 & 0 & 0 & I_{n-r_s} \end{array}\right]^T$ and $\overline{N}_{2,in}^1 = (M_{in}^T M_{in})^{-1} M_{in}^T\left[I - \overline{B}_{2,in}^1(\overline{C}_{in}\overline{B}_{2,in}^1)^{-1}\overline{C}_{in}\right]$, and show that it has all stable eigenvalues (see [16, Lemma 1] for a similar proof). The following Lemma states that ε_{max} in (27) is so designed such that L^* and S guarantee a SPR property. Proof of Lemma 1 is very similar to [16, Lemma 2] and therefore is omitted here.

Lemma 1. *Given Assumptions 1 to 6, the finite pair of $L^* \in \mathbb{R}^{n\times m}$ and $S \in \mathbb{R}^{m\times m}$ as in (26), with ϵ chosen in (27), guarantees that the transfer function $\{(A^* - L^*C), \overline{B}_2^{1*}, SC\}$ is strictly positive real.*

Define partition $S^T = \begin{bmatrix} S_2^T & S_1^T \end{bmatrix}$ with $S_2 \in \mathbb{R}^{m\times p}$ and $S_1 \in \mathbb{R}^{m_s\times p}$. Lemma 1 also implies that $\{(A^* - L^*C), B_2^{1*}, S_2C\}$ is also SPR.

F. Adaptive Law and Stability Proof

The structure of the SPR error model (33) suggests that the uncertainty estimates $\Psi_\Lambda(t)$ and $\Psi_m(t)$ should be adjusted using

$$\begin{aligned} \dot{\Psi}_\Lambda(t) &= -\Gamma_{\psi_\lambda}\chi e_y^T S_2^T \\ \dot{\Psi}_m(t) &= \Gamma_{\psi_m}\overline{e}_{ys} e_y^T S_2^T \end{aligned} \tag{35}$$

where $\Gamma_{\psi_\lambda} > 0$ and $\Gamma_{\psi_m} > 0$ are adaptation gains. The following theorem guarantees the stability and tracking performance of the adaptive system, whose proof can be found in Appendix B. Define $e_z(t) = z - z_m$ as tracking errors.

Theorem 1. *For an uncertain MIMO plant model (10) that satisfies Assumptions 1 to 6, and for any $z_{cmd}(t)$ that is piecewise continuous, the adaptive controller (17)(18)(19)(20)(35), with L and S designed in (26), guarantees that i) the closed-loop system has bounded solutions, ii) $e_y(t) \to 0$ as $t \to \infty$, and iii) $e_z(t) \to 0$ as $t \to \infty$.*

V. Applications to VFA

This section applies the adaptive controller with gain scheduling on a simple nonlinear VFA model. The model features three rigid wings hinged side-by-side (see [1]), which are allowed to rotate about the longitudinal axis (i.e. dihedral angle η). The platform features basic flexible wing effects and can be viewed as building blocks of large VFA. A 6-state nonlinear model has been developed in [1, Eq.s (45) and (46)] including aircraft's pitch mode and dihedral dynamics. Define α as the angle of attack, θ as pitch angle and q as pitch rate. The nonlinear model can be rewritten in the form of (3) with $\epsilon = \eta$ and $\beta = \begin{bmatrix} V & \alpha & q \end{bmatrix}^T$ as

$$\begin{bmatrix} d_3(\eta) & s\alpha c\eta & 0 & 0 \\ 0 & m & 0 & 0 \\ 0 & 0 & mV & 0 \\ 0 & 0 & 0 & c_1 + c_2 s^2\eta \end{bmatrix} \begin{bmatrix} \ddot{\eta} \\ \dot{V} \\ \dot{\alpha} \\ \dot{q} \end{bmatrix} + \begin{bmatrix} k_c - \frac{m^* s}{3} c\eta s\eta\dot{\eta} & \frac{m^* s}{2} c\eta c\alpha\dot{\alpha} & 0 & \frac{m^* s}{2} c\eta c\alpha \\ 0 & 0 & 0 & g \\ 0 & 0 & 0 & 0 \\ 2c_2 c\eta s\eta q & 3c_2 c\eta s\alpha\dot{\alpha} & 0 & 3c_2 c\eta s\alpha \end{bmatrix} \begin{bmatrix} \dot{\eta} \\ V \\ \alpha \\ q \end{bmatrix} + \begin{bmatrix} k_k & 0 & 0 & 0 \\ 0 & 0 & 0 & -g \\ 0 & 0 & 0 & 0 \\ 0 & 0 & 0 & 0 \end{bmatrix} \begin{bmatrix} \eta \\ \int V dt \\ \int \alpha dt \\ \theta \end{bmatrix} + \begin{bmatrix} c\eta s\eta & c\eta c\alpha \\ 0 & 0 \\ 0 & 0 \\ c\eta s\eta & c\eta s\alpha \end{bmatrix} \begin{bmatrix} \delta_e \\ \delta_a \end{bmatrix}, \quad (36)$$

where $s(\cdot) = sin(\cdot)$, $c(\cdot) = cos(\cdot)$ and δ_e and δ_a are properly scaled. Parameter c_1 and c_2 are inertia constants that depends on aircraft physical properties. d_3 is the rotation inertia about longitudinal axis and therefore a function of η. Measurements are vehicle vertical acceleration A_z, η and q. Other states, α and $\dot{\eta}$, are unmeasurable and are unavailable for control. The goal is to use center elevators δ_e and outer ailerons δ_a to track A_z command and regulate η.

The nonlinear model is linearized at 25 trim points defined by $V_0 = 30$ ft/sec, $\alpha_0 = 0$ deg, $\theta_0 = 0$ deg, $q = 0$ deg/sec, $\eta_0 \in [9, 11]^\circ$ with a step of 0.5, and $\dot{\eta}_0 \in [-0.2, 0.2]$ deg/sec with a step of 0.1. Example numerical values of the linearized model is shown in Eq.(37) for $\eta = 9^\circ$ and $\dot{\eta} = 0$ deg/sec. It is verified that the linearized model for $\eta = 9^\circ$ and $\dot{\eta} = 0.2$ deg/sec can be approximated as (8) using

$$\Theta_p^* = \begin{bmatrix} 0.006 & -4.52 & 0 & 0.005 & 0.041 & 1.47 \\ 0.001 & 1.83 & 0 & -0.002 & -0.035 & -0.59 \end{bmatrix}, \Lambda^* = \begin{bmatrix} 0.91 & 0.53 \\ 0.52 & 0.79 \end{bmatrix}$$

with a norm error of $2.6\% \|A_p\|$ and $1.8\% \|B_p\|$, respectively. The pitch mode of the VFA when $\eta \geq 10^\circ$ is unstable. For realistic simulation, (37) includes two first-order actuator dynamics with nominal time constant of 1 sec. u_e are elevator commands and u_a are aileron commands to the actuators.

For control design, first we designed control parameters for each trim. For example, L and S_2 using (26) and (23) with $a_1^1 = 0.2$, $a_1^0 = 1$, $\varepsilon = 100$, $\Lambda_{max} = 2$ and $\Psi_{max} = 30$ for the linearized model (37) is:

$$L = \begin{bmatrix} -34.23 & 64.10 & 49.35 \\ -11.54 & 55.96 & 2.23 \\ -5.46 & 31.86 & -2.82 \\ 60.32 & -11.47 & -33.51 \\ -49.09 & 286.3 & -25.20 \\ -0.118 & 20.27 & -2.26 \\ 30.12 & -716 & 21.78 \\ 45.32 & 138.9 & -72.34 \\ -4.88 & 28.50 & -2.51 \\ -50.70 & -45.95 & 218 \end{bmatrix}, \quad S_2 = \begin{bmatrix} -0.817 & 0 & -0.585 \\ 0.585 & 0 & -0.811 \end{bmatrix}. \quad (38)$$

Then we schedule the control parameters using real-time η measurements. For the baseline controller without adaptation terms, i.e. $\Psi_\Lambda(t) \equiv 0$ and $\Psi_m(t) \equiv 0$, the resulting controller is an observer-based gain scheduling linear controller (referred as the baseline controller) and the CRM acts as an observer. Performing frequency domain analysis [10, Chapter 5], as shown in the Figure 3 for $\eta = 9^\circ$, indicates that the baseline controller has adequate stability margins and small output sensitivity; the gain margin is $[-15.7,\ 27.1]dB$ and the phase margin is $\pm 57.1^\circ$.

The time domain simulation results with the nonlinear VFA model are shown in Figure 1. Two actuator models were simulated, one with a time constant of 1.5 second, and the other 4 second. Two adaptive controllers were tested: one is relative degree one as developed in Ref. [14], which pretends the actuator dynamics is not present; the other is the relative degree two shown in Section IV based on a nominal actuator model as in (37). The baseline controller was also tested. With fast actuators, both adaptive controllers were able to achieve tracking goals while the baseline controller failed to do so, as shown in Figure 1a. When actuator dynamics was slow as shown in Figure 1, only relative degree two adaptive controller can achieve stable command tracking after 3 step commands. The parameter trajectories of the relative degree two adaptive controller are shown in Figure 2.

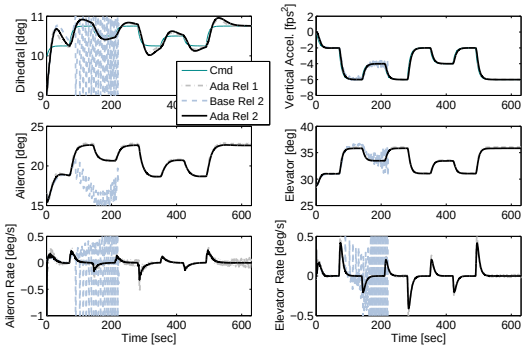

(a) Actuators with a time constant of 1.5 sec

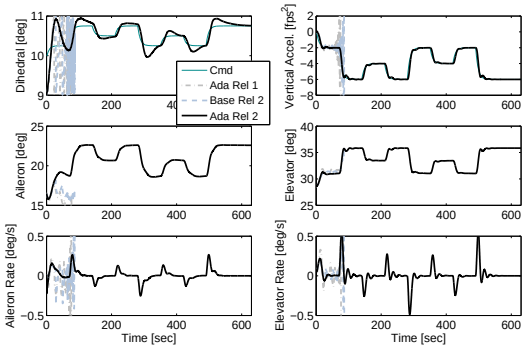

(b) Actuators with a time constant of 4 sec

Fig. 1: The tracking of η and A_z using the relative degree two adaptive controller, compared with the relative degree one adaptive controller and the baseline controller

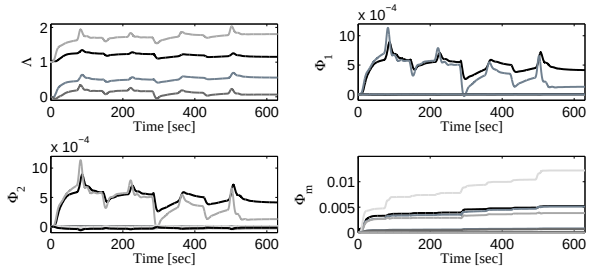

Fig. 2: The parameter trajectories of the relative degree two adaptive controller in the simulation shown in Figure 1b

$$\begin{bmatrix} \dot{V} \\ \dot{\alpha} \\ \dot{\theta} \\ \dot{q} \\ \dot{\eta} \\ \ddot{\eta} \\ \dot{\delta}_e \\ \dot{\delta}_a \\ \dot{w}_\eta \\ \dot{w}_{A_z} \end{bmatrix} = \underbrace{\begin{bmatrix} -0.279 & 3.476 & -32.2 & -0.015 & 0.514 & 0.525 & -2.57 & -6.47 & 0 & 0 \\ -0.070 & -4.104 & 0 & 1.013 & 0.193 & 0.100 & -0.795 & -0.079 & 0 & 0 \\ 0 & 0 & 0 & 1 & 0 & 0 & 0 & 0 & 0 & 0 \\ 0 & -54.04 & 0 & 0.255 & 1.845 & 21.41 & 5.991 & -6.363 & 0 & 0 \\ 0 & 0 & 0 & 0 & 0 & 1 & 0 & 0 & 0 & 0 \\ 0.002 & 0.044 & 0 & 0.819 & -0.075 & -6.518 & 0.195 & -0.034 & 0 & 0 \\ 0 & 0 & 0 & 0 & 0 & 0 & -1 & 0 & 0 & 0 \\ 0 & 0 & 0 & 0 & 0 & 0 & 0 & -1 & 0 & 0 \\ 0 & 0 & 0 & 1 & 0 & 0 & 0 & 0 & 0 & 0 \\ 0 & -123.12 & 0 & 0 & 0 & 0 & -23.84 & -2.376 & 0 & 0 \end{bmatrix}}_{A} \underbrace{\begin{bmatrix} V \\ \alpha \\ \theta \\ q \\ \eta \\ \dot{\eta} \\ \delta_e \\ \delta_a \\ w_\eta \\ w_{A_z} \end{bmatrix}}_{x} + \underbrace{\begin{bmatrix} 0 & 0 \\ 0 & 0 \\ 0 & 0 \\ 0 & 0 \\ 0 & 0 \\ 0 & 0 \\ 1 & 0 \\ 0 & 1 \\ 0 & 0 \\ 0 & 0 \end{bmatrix}}_{B_2} \underbrace{\begin{bmatrix} u_e \\ u_a \end{bmatrix}}_{u} + \underbrace{\begin{bmatrix} 0 & 0 \\ 0 & 0 \\ 0 & 0 \\ 0 & 0 \\ 0 & 0 \\ 0 & 0 \\ 0 & 0 \\ 0 & 0 \\ -1 & 0 \\ 0 & -1 \end{bmatrix}}_{B_z} \underbrace{\begin{bmatrix} z_q \\ z_{A_z} \end{bmatrix}}_{z_{cmd}}$$

$$y = \begin{bmatrix} q \\ w_\eta \\ w_{A_z} \end{bmatrix} = \underbrace{\begin{bmatrix} 0 & 0 & 0 & 1 & 0 & 0 & 0 & 0 & 0 & 0 \\ 0 & 0 & 0 & 0 & 0 & 0 & 0 & 0 & 1 & 0 \\ 0 & 0 & 0 & 0 & 0 & 0 & 0 & 0 & 0 & 1 \end{bmatrix}}_{C} x \tag{37}$$

Suppose we freeze the adaptive parameters $\Psi_\Lambda(t)$ and $\Psi_m(t)$ at the end of the simulation, the resulting "snapshot" closed-loop systems consist of a uncertain LTI plant and a linear observer-based controllers. The frequency response of the snapshot system shows that the adaptation improves the robustness of the system, as shown in Figure 3. At the beginning of the simulation, the uncertain closed-loop system only has a gain margin of $[-4.0, 4.6]dB$ and the phase margin of $\pm 23.8°$. After adaptation, the gain margin recovers to $[-7.9, 12.6]dB$ and phase margin to $\pm 41.6°$.

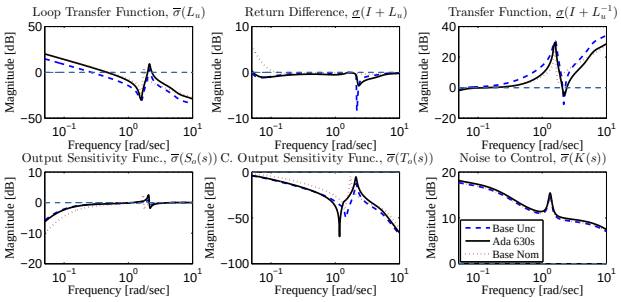

Fig. 3: The frequency domain analysis of the snapshot closed-loop system shows that adaptation mitigates the effects of model uncertainties on system's robustness

VI. Conclusions

To accommodate parametric uncertainties in a class of multi-input-multi-output plants motivated by very flexible aircraft, this paper develops a new adaptive output feedback controller that includes a baseline controller based on observers and parameter adaptation based on a closed-loop reference model. In particular, the new control design allows the underlying plant model to have more outputs than inputs, and have first-order actuator dynamics and a large class of uncertainties. Control parameters are designed such that this controller can guarantee global stability and asymptotic tracking, The overall design is validated using simulations on a nonlinear VFA model navigating through multiple trims.

References

[1] T. Gibson, A. Annaswamy, and E. Lavretsky, "Modeling for Control of Very Flexible Aircraft," in *AIAA, Guidance, Navigation, and Control Conferences*, 2011.

[2] C. Shearer and C. Cesnik, "Nonlinear Flight Dynamics of Very Flexible Aircraft," *AIAA Journal of Aircraft*, vol. 44, pp. 1528–1545, 2005.

[3] T. E. Noll, J. M. Brown, M. E. Perez-Davis, S. D. Ishmael, G. C. Tiffany, and M. Gaier, "Investigation of the Helios Prototype Aircraft Mishap Volume I: Mishap Report," *NASA*, 2004.

[4] C. Shearer and C. Cesnik, "Trajectory Control of Very Flexible Aircraft," *AIAA Guidance, Navigation, and Control Conference and Exhibit*, 2006.

[5] W. Su, "Coupled nonlinear aeroelasticity and flight dynamics of fully flexible aircraft," Ph.D, University of Michigan, Ann Arbor, 2008.

[6] K. S. Narendra and A. M. Annaswamy, *Stable adaptive systems*. Dover Publications, 2004.

[7] G. Tao, *Adaptive control design and analysis*. Hoboken, N.J.: Wiley-Interscience, 2003.

[8] A. S. Morse, "Parameterizations for multivariable adaptive control," in *Proceedings of the 20th IEEE Conference on Decision and Control including the Symposium on Adaptive Processes*. New York, NY, USA: IEEE, 1981, pp. 970–972.

[9] R. P. Singh and K. S. Narendra, "Prior information in the design of multivariable adaptive controllers," *IEEE Transactions on Automatic Control*, vol. AC-29, no. 12, p. 1108, 1984.

[10] E. Lavretsky and K. A. Wise, *Robust and adaptive control: with aerospace applications*. London ; New York: Springer, 2013.

[11] Z. Qu, E. Lavretsky, and A. M. Annaswamy, "An Adaptive Controller for Very Flexible Aircraft," in *AIAA, Guidance, Navigation, and Control Conferences*, 2013, pp. 10.2514/6.2013–4854.

[12] T. E. Gibson, Z. Qu, A. M. Annaswamy, and E. Lavretsky, "Adaptive Output Feedback Based on Closed-Loop Reference Models," *IEEE Transactions Automatic Control*, vol. PP, no. 99, p. 1, 2015.

[13] D. P. Wiese, A. M. Annaswamy, J. A. Muse, M. A. Bolender, and E. Lavretsky, "Adaptive Output Feedback Based on Closed-Loop Reference Models for Hypersonic Vehicles," in *AIAA Guidance, Navigation, and Control Conference (To Appear)*, 2015, pp. 10.2514/6.2015–1755.

[14] Z. Qu and A. M. Annaswamy, "Adaptive Output-Feedback Control with Closed-Loop Reference Models for Very Flexible Aircraft," *AIAA, Journal of Guidance, Control, and Dynamics (preprint in MIT dSpace)*, 2015.

[15] T. E. Gibson, A. M. Annaswamy, and E. Lavretsky, "On Adaptive Control With Closed-Loop Reference Models: Transients, Oscillations, and Peaking," *Access, IEEE*, vol. 1, pp. 703–717, 2013.

[16] Z. Qu, A. M. Annaswamy, and E. Lavretsky, "Adaptive Output-Feedback Control for Relative Degree Two Systems Based on Closed-Loop Reference Models," in *IEEE 54th Conference on Decision and Control*, Osaka, Japan, 2015.

[17] A. G. J. MacFarlane and N. Karcanias, "Poles and zeros of linear multivariable systems : a survey of the algebraic, geometric and complex-variable theory," *International Journal of Control*, vol. 24, no. 1, pp. 33–74, 1976.

[18] W. J. Rugh and J. S. Shamma, "Research on gain scheduling," *Automatica*, vol. 36, no. 10, pp. 1401–1425, 2000.

[19] B. Kouvaritakis and A. G. J. MacFarlane, "Geometric approach to analysis and synthesis of system zeros. II. Non-square systems," *International Journal of Control*, vol. 23, no. 2, pp. 167–181, 1976.

[20] J. Doyle and G. Stein, "Multivariable feedback design: Concepts for a classical/modern synthesis," *Automatic Control, IEEE Transactions on*, vol. 26, no. 1, pp. 4–16, 1981.

[21] Z. Qu, A. M. Annaswamy, and E. Lavretsky, "Squaring-Up Method for Relative Degree Two Plants," in *MIT dSpace Archive*, 2015.

[22] M. Mueller, "Output feedback control and robustness in the gap metric," Ph.D Dissertation, Universitätsverlag Ilmenau, 2009.

APPENDIX

A. Linearization of VFA Model

Define $(\cdot)_{/[\cdot]_0} = \frac{\partial(\cdot)}{\partial[\cdot]}\Big|_{[\cdot]_0}$ as partial differential variables. Linearizing (3) around a trim point $\begin{bmatrix} \ddot{\epsilon}_0 & \dot{\epsilon}_0 & \epsilon_0 & \dot{\beta}_0 & \beta_0 & \lambda_0 & u_0 \end{bmatrix}^T$ yields

$$\begin{aligned}
&\left(\underbrace{\begin{bmatrix} I & 0 & 0 \\ 0 & (M_{FF})_{\epsilon_0} & (M_{FB})_{\epsilon_0} \\ 0 & (M_{BF})_{\epsilon_0} & (M_{BB})_{\epsilon_0} \end{bmatrix}}_{Q_1} + \underbrace{\begin{bmatrix} 0 & 0 & 0 \\ 0 & \Delta M_{FF} & \Delta M_{FB} \\ 0 & \Delta M_{BF} & \Delta M_{BB} \end{bmatrix}}_{\Delta Q_1}\right)\begin{bmatrix} \dot{\epsilon} \\ \ddot{\epsilon} \\ \dot{\beta} \end{bmatrix} \\
&= \Bigg(\underbrace{\begin{bmatrix} 0 & I & 0 \\ -(K_{FF})_{\epsilon_0} + (J_{h\epsilon}^T)_{\epsilon_0} F^{aero}_{/\epsilon_0} & -C_e & (J_{h\epsilon}^T)_{\epsilon_0} F^{aero}_{/\beta_0} \\ 0 & 0 & -C_{RB} + (J_{hb}^T)_{\epsilon_0} F^{aero}_{/\beta_0} \end{bmatrix}}_{Q_2} \\
&\quad + \underbrace{\begin{bmatrix} 0 & 0 & 0 \\ \Delta K_{FF} & \Delta C_{FF} & \Delta C_{FB} \\ \Delta K_{BF} & \Delta C_{BF} & \Delta C_{BB} \end{bmatrix}}_{\Delta Q_2}\Bigg)\underbrace{\begin{bmatrix} \epsilon \\ \dot{\epsilon} \\ \beta \end{bmatrix}}_{x_p} + \underbrace{\begin{bmatrix} 0 \\ B_{F/u_0} \\ B_{B/u_0} \end{bmatrix}}_{Q_3} u_p
\end{aligned} \tag{39}$$

where

$$\begin{aligned}
\Delta M_{FF} &= -(J_{h\epsilon}^T)_{\epsilon_0} F^{aero}_{/\dot{\epsilon}_0} & \Delta M_{FB} &= -(J_{h\epsilon}^T)_{\epsilon_0} F^{aero}_{/\beta_0} \\
\Delta M_{BF} &= -(J_{hb}^T)_{\epsilon_0} F^{aero}_{/\dot{\epsilon}_0} & \Delta M_{BB} &= -(J_{hb}^T)_{\epsilon_0} F^{aero}_{/\beta_0} \\
\Delta B_{F/\lambda_0} &= (J_{h\epsilon}^T)_{\epsilon_0} F^{aero}_{/\lambda_0} & \Delta B_{B/\lambda_0} &= (J_{hb}^T)_{\epsilon_0} F^{aero}_{/\lambda_0} \\
\Delta K_{FF} &= M_{FF/\epsilon_0}\ddot{\epsilon}_0 + M_{FB/\epsilon_0}\dot{\beta}_0 \\
\Delta K_{BF} &= M_{BF/\epsilon_0}\ddot{\epsilon}_0 + M_{BB/\epsilon_0}\dot{\beta}_0 \\
\Delta C_{FF} &= -(C_{FF})_{x_0} - C_{FF/\dot{\epsilon}_0}\dot{\epsilon}_0 - C_{FB/\dot{\epsilon}_0}\beta_0 + (J_{h\epsilon}^T)_{\epsilon_0} F^{aero}_{/\dot{\epsilon}_0} \\
\Delta C_{BF} &= -(C_{BF})_{x_0} - C_{BF/\dot{\epsilon}_0}\dot{\epsilon}_0 - C_{BB/\dot{\epsilon}_0}\beta_0 + (J_{hb}^T)_{\epsilon_0} F^{aero}_{/\dot{\epsilon}_0} \\
\Delta C_{FB} &= -(C_{FB})_{x_0} - C_{FF/\beta_0}\dot{\epsilon}_0 - C_{FB/\beta_0}\beta_0 \\
\Delta C_{BB} &= -(C_{BB})_{x_0} - C_{BF/\beta_0}\dot{\epsilon}_0 - C_{BB/\beta_0}\beta_0
\end{aligned} \tag{40}$$

$B_{F/u_0} = (J_{h\epsilon}^T)_{\epsilon_0} F^{aero}_{/u_0}$ and $B_{B/u_0} = (J_{hb}^T)_{\epsilon_0} F^{aero}_{/u_0}$. Without loss of generality, we scale each input so that $F^{aero}_{/u_0} = I$. In realistic application, only $\begin{bmatrix} \epsilon_0 & \beta_0 & u_0 \end{bmatrix}^T$ can be measured accurately and therefore variables that depend on them can be gain scheduled. $\begin{bmatrix} \dot{\epsilon}_0 & \ddot{\epsilon}_0 & \dot{\beta}_0 & \lambda_0 \end{bmatrix}^T$ cannot be measured accurately and therefore variables that depends on them are generally unknown. As a result, Q_1, Q_2 and Q_3 are known but ΔQ_1 and ΔQ_2 are unknown. Examination on (40) using (4) reveals that

$$\Delta Q_1 = \begin{bmatrix} 0 \\ J_{h\epsilon}^T \\ J_{hb}^T \\ 0 \end{bmatrix}_{\epsilon_0} \underbrace{\begin{bmatrix} 0 & F^{aero}_{/\ddot{\epsilon}_0} & F^{aero}_{/\dot{\beta}_0} & 0 \end{bmatrix}}_{\Theta_{q_1}^{*T}} = Q_3\Theta_{q_1}^{*T} \tag{41}$$

and

$$\begin{aligned}
\Delta Q_2 &= \begin{bmatrix} 0 \\ J_{h\epsilon}^T \\ J_{hb}^T \end{bmatrix}_{\epsilon_0} \underbrace{\begin{bmatrix} M_e\left(\frac{\partial J_{h\epsilon}}{\partial \epsilon}\ddot{\epsilon} + \frac{\partial J_{hb}}{\partial \epsilon}\beta\right) & M_e\left(j_{h\epsilon} + \frac{\partial j_{h\epsilon}}{\partial \dot{\epsilon}}\dot{\epsilon} + \frac{\partial j_{hb}}{\partial \dot{\epsilon}}\beta\right) \\ M_e\left(j_{hb} + \frac{\partial j_{h\epsilon}}{\partial \dot{\beta}}\dot{\epsilon} + \frac{\partial j_{hb}}{\partial \dot{\beta}}\beta\right) \end{bmatrix}_{x_0}}_{\Theta_{q_2}^{*T}} \\
&= Q_3\Theta_{q_2}^{*T}
\end{aligned} \tag{42}$$

which leads to a plant model with modeled uncertainties as

$$\left(Q_1 + Q_3\Theta_{q_1}^{*T}\right)\dot{x}_p = \left(Q_2 + Q_3\Theta_{q_2}^{*T}\right)x_p + Q_3 u_p. \tag{43}$$

Assume that Q_1, $(Q_1 + Q_3\Theta_{q_1}^{*T})$ and $(I + \Theta_{q_2}^{*T}Q_1^{-1}Q_3)$ are invertible around the equilibrium. Taking inverse on both sides, and noting

$$(Q_1 + Q_3\Theta_{q_1}^{*T})^{-1} = Q_1^{-1} - Q_1^{-1}Q_3\underbrace{(I + \Theta_{q_1}^{*T}Q_1^{-1}Q_3)^{-1}\Theta_{q_1}^{*T}}_{\overline{\Theta}_{q_1}^{*T}}Q_1^{-1} \tag{44}$$

yields

$$\begin{aligned}
\dot{x}_p &= \left(Q_1^{-1} - Q_1^{-1}Q_3\overline{\Theta}_{q_1}^{*T}Q_1^{-1}\right)\left(Q_2 + Q_3\Theta_{q_2}^{*T}\right)x_p \\
&\quad + \left(Q_1^{-1} - Q_1^{-1}Q_3\overline{\Theta}_{q_1}^{*T}Q_1^{-1}\right)Q_3 u_p \qquad (45) \\
&= \left[Q_1^{-1}Q_2 + Q_1^{-1}Q_3\left(\Theta_{q_2}^{*T} - \overline{\Theta}_{q_1}^{*T}Q_1^{-1}Q_2 - \overline{\Theta}_{q_1}^{*T}Q_1^{-1}Q_3\Theta_{q_2}^{*T}\right)\right]x_p \qquad (46) \\
&\quad + Q_1^{-1}Q_3\left(I - \overline{\Theta}_{q_1}^{*T}Q_1^{-1}Q_3\right)u_p \\
&= \left[\underbrace{A_p + B_p\left(\Theta_{q_2}^{*T} - \overline{\Theta}_{q_1}^{*T}A_p - \overline{\Theta}_{q_1}^{*T}B_p\Theta_{q_2}^{*T}\right)}_{\Lambda^*\Theta_p^{*T}}\right]x_p + B_p\underbrace{\left(I - \overline{\Theta}_{q_1}^{*T}B_p\right)}_{\Lambda^*}u_p \qquad (47)
\end{aligned}$$

with $A_p = Q_1^{-1}Q_2$, $B_p = Q_1^{-1}Q_3$.

B. Proof of Theorem 1

Proof. We propose a Lyapunov function candidate

$$\begin{aligned}
V &= e_{mx}^T P^* e_{mx} \\
&\quad + Tr\left[\widetilde{\Psi}_\Lambda^T\Gamma_{\psi_\lambda}^{-1}\Lambda^*\widetilde{\Psi}_\Lambda\right] + Tr\left[\widetilde{\Psi}_m^T\Gamma_{\psi_m}^{-1}\widetilde{\Psi}_m\right]
\end{aligned} \tag{48}$$

where $P^* = T_{in}^T P_{in}^* T_{in}$ is the matrix that guarantees the SPR properties of $\{A_{L^*}^*, \overline{B}_2^{1*}, SC\}$, satisfying

$$P^*A_{L^*}^* + A_{L^*}^{*T}P^* = -\overline{Q}^* < 0 \tag{49}$$

$$P^*\overline{B}_2^{1*} = C^T S^T, \tag{50}$$

where $\overline{Q}^* = Q^* + \bar{C}^T R_{in}^{-1}\bar{C} > 0$ with $Q^* = T_{in}^T Q_{in}^* T_{in}$. Partition on both sides of (50) yields

$$P^*\left[B_2^{1*}B_1\right] = C^T\begin{bmatrix} S_2^T & S_1^T \end{bmatrix}. \tag{51}$$

By appealing to (33)(34)(35)(49)(51), the derivative of V has the following bound

$$\begin{aligned}
\dot{V} &= e_{mx}^T\left[A_{L^*}^{*T}P^* + P^*A_{L^*}^*\right]e_{mx} \\
&\quad - 2e_{mx}^T[P^*B_2^{1*} - C^T S_2^T]\Lambda^*\widetilde{\Psi}_\Lambda^T\overline{\chi} \\
&\quad - 2e_{mx}^T[P^*B_2^{1*} - C^T S_2^T]\widetilde{\Psi}_m^T\overline{e}_{ys} \\
&= -e_{mx}^T\overline{Q}^* e_{ux} \le 0.
\end{aligned} \tag{52}$$

Then $e_{mx}(t)$, $\widetilde{\Psi}_\Lambda(t)$ and $\widetilde{\Psi}_m(t)$ are bounded as $t \to \infty$, which proves i). Applying Barbalat's Lemma shows that $e_{mx}(t) \to 0$ as $t \to \infty$, which proves ii). From (34) and (22), the fact $e_{mx}(t) \to 0$ implies that $e_y(t) \to 0$, $e_{ys}(t) \to 0$ and $\overline{e}_{ys}(t) \to 0$ as $t \to \infty$, which in turn implies that x_m, as well as $\overline{x}_m$ and $\overline{u}_{bl}$, is bounded. Further, define $e_{pz}(t) = z - z_{cmd}$ and

$$e_{mz}(t) = z_m - z_{cmd} + B_{2,I}\left(a_1^1 s + a_1^0\right)\left(\Psi_m^T(t)\overline{e}_{ys}\right) + L_I e_y, \tag{53}$$

where $B_{2,I}$ and L_I are rows of B_2 and L corresponding to the integral errors, respectively. From (9), it is noted that $\int e_{pz}(t)dt$ is an element of x and $\int e_{mz}(t)dt$ is an element of x_m. As a result, $e_{mx}(t) \to 0$ as $t \to \infty$, together of the definition of $e_{mx}(t)$ as in (32), implies

$$\begin{aligned}
\int e_z(t)dt \to &-B_{2,I}\int\left[\left(a_1^1 s + a_1^0\right)\left(\Psi_m^T(t)\overline{e}_{ys}\right)\right]dt \\
&+ B_{2,I}\Lambda_2^* a_1^1\widetilde{\Psi}_\Lambda^T\overline{\chi} - B_{2,I}a_1^1(\widetilde{\Psi}_m^T(t)\overline{e}_{ys}).
\end{aligned} \tag{54}$$

Therefore, $\int e_z(t)dt$ is bounded as $t \to \infty$. Further, $\dot{e}_z(t)$ is bounded as $t \to \infty$. Applying Barbalat's Lemma shows that $e_z(t) \to 0$ as $t \to \infty$, which proves iii).